Vibrations of Magnetic Origin of Switched Reluctance Motors

Lieven Vandevelde[1], Johan J. C. Gyselinck[2], Francis Bokose[1], and Jan A. A. Melkebeek[1]

[1] Electrical Energy Laboratory (EELAB)
Dept. of Electrical Energy, Systems and Automation (EESA), Ghent University
Sint-Pietersnieuwstraat 41, B-9000 Gent, Belgium
tel. +32 9 264 34 22 – fax +32 9 264 35 82
e-mail: lieven.vandevelde@rug.ac.be

[2] Dept. of Electrical Engineering (ELAP)
Montefiore Institute, University of Liège
Sart-Tilman, Bât. B 28, B - 4000 Liège, Belgium
tel + 32 4 366 37 32 – fax + 32 4 366 29 10
e-mail : johan.gyselinck@ulg.ac.be

Abstract – **Vibrations and acoustic noise are some of the fundamental problems in the design and exploitation of switched reluctance motors (SRM). Adequate experimental and analysis methods may help to resolve these problems. This paper presents a theoretical analysis of the magnetic force distribution in switched reluctance motors and a procedure for calculating the magnetic forces and the resulting vibrations based on the 2D finite element method. Magnetic field and force computations and a structural analysis of the stator have been carried out in order to compute the frequency spectrum of the generalized forces and displacements of the most relevant vibration modes. It is shown that for these vibration modes, the frequency spectrum can be predicted analytically.**

The theoretical and the numerical analyses have been applied to a 6/4 SRM and an experimental validation is presented.

1. Introduction

The main sources of vibration and noise in switched reluctance motors (SRM) have been highlighted in earlier publications [1, 2]. Experiments have been carried out on existing SRMs of various configurations to identify the factors which affect the production of vibration and noise [1, 3]. It is an established fact that the main contributors to vibration and noise in SRMs are sources of magnetic origin. All mechanical components of the machine contribute to vibration and noise in varying degrees and are supposed to be modelled. However, the deformation of the stator lamination stack due to magnetic forces is the main source of vibrations and noise in switched reluctance motors [1, 3, 4]. These sources are affected by the control strategy used and are characterized by complex wave patterns. The odd harmonics of these waves excite more vibrations and noise than the even harmonics [5]. It is due to this complexity that proper analytical as well as 2D/3D finite element electromagnetic and structural analysis are required. However, in a comparative finite element analysis of modes and frequencies of 2D and 3D SRM stator structures, it was shown that 2D finite element analysis of vibrations and noise in the stator structures is adequate, and that the error is only about 15% [5].

The aim of this paper is to contribute to both the theoretical and the numerical analysis of vibrations of magnetic origin of the SRM.

First, the exciting magnetic forces are studied with respect to their distribution in time and space by determining the time harmonic and spatial orders of the forces. This analysis includes the effects of possible anomalies (asymmetries) of the SRM, the converter and the load.

Further, a 2D finite element (FE) procedure for calculating the vibrations is presented, which is based on a novel force calculation method [7] and on the modal superposition technique [6]. By considering the vibrations as rotating waves, the frequency spectrum and the direction of rotation of the waves can be predicted on the basis of the theoretical analysis.

The theoretical and the numerical analyses have been applied to a 6/4 SRM and the results are compared with vibration measurements at different load conditions.

2. Theoretical Analysis
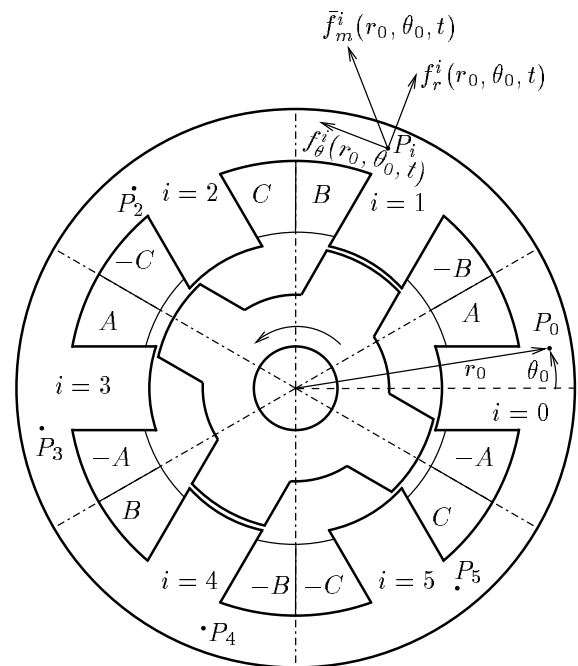
Fig. 1. Cross section of a 6/4 SRM

For the theoretical analysis of the magnetic forces acting

on the stator of a switched reluctance motor and the ensuing deformation, we divide the stator cross section into N_s sectors, $i=0, \ldots, N_s$-1, with N_s the number of stator poles, as illustrated in Fig. 1 for a 6/4 SRM. We further consider a point P_0 in the zeroth sector and the corresponding points – i.e. with the same relative position – in the other sectors. The magnetic force density $\bar{f}_m$ and the displacement $\bar{u}$ in this set of N_s points can be resolved into a series of components with time harmonic orders λ_k and spatial orders κ_k. For example, the radial magnetic force f_r^i in the points P_i ($i=0, \ldots, N_s$-1) can be written as

$$f_r^i(r_0, \theta_0, t) = \sum_k \Re\left[\bar{F}_{rk}(\theta_0, r_0) e^{j\left(\lambda_k 2\pi f_{rot} t - \kappa_k \frac{2\pi}{N_s} i\right)} \right]$$

(1)

where f_{rot} is the rotor speed (in Hz), r_0 and θ_0 are the polar coordinates of the point P_0 in the zeroth sector. The direction of increasing i corresponds with the direction of rotation, which is chosen anticlockwise.

Two components with time harmonic and spatial orders (λ_k,κ_k) and (λ_l,κ_l) respectively, are equivalent if

$$(\lambda_k, \kappa_k) = \pm(\lambda_l, \kappa_l + mN_s) \quad (m : \text{integer}) . \quad (2)$$

Therefore the following constraints can be imposed on the orders:

$$\lambda_k \geq 0 \quad (3)$$

$$\begin{cases} \text{if } \lambda_k = 0 \quad : \quad 0 \leq \kappa_k \leq \frac{N_s}{2} \\ \text{if } \lambda_k > 0 \quad : \quad -\frac{N_s}{2} + 1 \leq \kappa_k \leq \frac{N_s}{2} \end{cases} \quad (4)$$

In this case, the sign of the spatial order κ_k determines the direction of rotation of the component, viz the same direction as the rotor for positive orders and the opposite direction for negative orders.

In the following paragraphs the orders (λ_k,κ_k) of the force components will be discussed in case of a 6/4 SRM.

A. Main force components

Firstly, we consider an idealized SRM drive, i.e. we assume that the SRM and its power electronic supply are completely symmetrical and that the load torque is constant, whereas the speed may fluctuate due to the electromagnetic torque ripple of the SRM. Under these conditions, the working principle of the 6/4 SRM leads to the following periodicities in time and space of both radial and tangential magnetic force densities f_r and f_θ:

$$f^i(r_0, \theta_0, t) = f^{i+1}(r_0, \theta_0, t - \frac{1}{12f_{rot}}) \quad (5)$$

$$f^i(r_0, \theta_0, t) = f^i(r_0, \theta_0, t - \frac{1}{4f_{rot}}) \quad (6)$$

On the basis of these periodicity conditions (5)-(6), it can easily be shown that the time and space harmonic orders, λ_k and κ_k, are bound by the following restrictions:

$$\begin{cases} \lambda_k = 4(3m - n) \\ \kappa_k = 2n \end{cases} \quad (m, n : \text{integer}) \quad (7)$$

We remark that the spatial orders are even and that the time harmonics are quadruples, i.e. the fundamental frequency of the forces is the drive frequency $f_0 = 4f_{rot}$.

According to (7) and (4), with N_s=6, the main magnetic force components, i.e. for an idealized 6/4 SRM drive, are determined by:

$$\begin{array}{llll} \kappa_k = 0 & : & \lambda_k = 4(3m) & = 0, 12, 24, \ldots \\ \kappa_k = 2 & : & \lambda_k = 4(3m - 1) & = 8, 20, 32, \ldots \\ \kappa_k = -2 & : & \lambda_k = 4(3m + 1) & = 4, 16, 28, \ldots \end{array}$$

(8)

B. Side bands

Load torque ripples and possible asymmetries of the SRM and the converter may cause additional components or 'side bands' to the main components (8).

As the fundamental frequency of the phase currents is the drive frequency $f_0 = 4f_{rot}$ and as each phase winding A, B and C consists of a pair of coils wound around diametrically opposed poles and connected in series, asymmetries of the converter are characterized by the following orders (λ_k',κ_k'):

$$\begin{cases} \lambda_k' = 4\sigma_1 \\ \kappa_k' = 2\sigma_2 \end{cases} \quad (\sigma_1, \sigma_2 : \text{integer}) \quad (9)$$

The orders of asymmetries of the stator geometry and of static rotor eccentricity (i.e. eccentricity of the shaft and the stator) are given by:

$$\begin{cases} \lambda_k' = 0 \\ \kappa_k' = \varepsilon_s \end{cases} \quad (\varepsilon_s : \text{integer}) \quad (10)$$

In a reference frame fixed to the stator, the asymmetries of the rotor geometry, such as dynamic rotor eccentricity (i.e. eccentricity of the shaft and the rotor core), feature the following orders:

$$\begin{cases} \lambda_k' = \varepsilon_r \\ \kappa_k' = \varepsilon_r \end{cases} \quad (\varepsilon_r : \text{integer}) \quad (11)$$

As the torque corresponds to tangential force components of zeroth spatial order, load torque ripples are characterized by the following orders:

$$\begin{cases} \lambda_k' = \tau \\ \kappa_k' = 0 \end{cases} \quad (12)$$

C. General expression of the time harmonic and spatial orders

The magnetic forces in an actual SRM are found by 'modulating' the forces in an idealized SRM with the anomalies mentioned above. The general expression of the time harmonic and spatial orders of the magnetic force distribution is thus found by adding the orders (λ_k',κ_k') (9)-(12) to the orders of the main components (λ_k,κ_k) (8):

$$\begin{cases} \lambda_k = 4(3m - n) + 4\sigma_1 + \varepsilon_r + \tau \\ \kappa_k = 2n + 2\sigma_2 + \varepsilon_s + \varepsilon_r \end{cases} \quad (13)$$

Analogously, the vibrations of magnetic origin are characterized by the orders (λ_k,κ_k) (13). In this respect, we remark
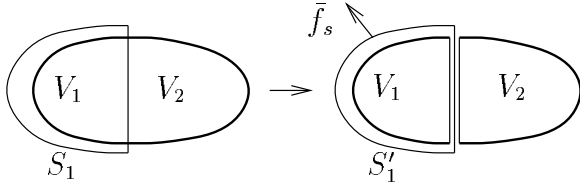
Fig. 2. Definition of long-range magnetic forces

a. Magnetic flux pattern

b. Magnetic force distribution and deformation

c. Magnetic flux and force distribution in a stator pole

Fig. 3. Some results of a static 2D FE calculation

that mechanical asymmetries of the SRM, which may cause a discrepancy between the orders of the exciting force component and those of the resulting vibration component(s), are already included in (13), viz via the term ε_s.

The expression of the orders (λ_k, κ_k) (13) can be used for predicting the frequency spectrum of the vibrations (and thus the noise) of SRM's and for determining the origin of experimentally observed or computed frequency components.

3. Numerical Analysis

A. Magnetic Force Calculation

For calculating the magnetic force distribution, an original method, presented by the authors in previous papers [7, 8], is used. The method is based on the separation of the forces in a magnetized elastic material into magnetic long-range forces and short-range forces or stresses. The latter represent mechanical stresses as well as magnetic short-range forces, i.e. local interactions (magnetostriction).

As illustrated in Fig. 2, the long-range magnetic force acting on a part V_1 inside the surface S_1 of a magnetic body is defined as the force acting on it when separated from the rest of the magnetic material (V_2) by means of an imaginary gap of infinitesimal width. This way, the short-range forces (i.e. the interactions on a microscopic scale) between the material in V_1 and V_2 vanish. The long-range force $\bar{F}$ on the material in V_1 can be calculated by integrating the Maxwell stresses $\bar{f}_s$ over the surface S_1'. On the basis of this definition, the deformation due to the long-range magnetic forces can be calculated by means of the following (fictitious) magnetic force density $\bar{f}_m^*$ (N/m³) [7, 8] :

$$\bar{f}_m^* = \bar{\nabla} \cdot \bar{\bar{T}}_m^* , \tag{14}$$

$$\bar{\bar{T}}_m^* = \bar{B}\bar{H} - \frac{\mu_0}{2}H^2\bar{\bar{I}} + \frac{\mu_0}{10}M^2\bar{\bar{I}} + \frac{\mu_0}{5}\bar{M}\bar{M} , \tag{15}$$

which features a singularity at material boundaries, viz a surface force density $\bar{T}_m^*$ (N/m²) given by

$$\bar{T}_m^* = \frac{\mu_0}{2}M_n^2\bar{n} - \bar{n} \cdot \left(\frac{\mu_0}{10}M^2\bar{\bar{I}} + \frac{\mu_0}{5}\bar{M}\bar{M} \right) , \tag{16}$$

where $\bar{n}$ and M_n are the outward normal unit vector on the surface and the normal component of the magnetisation respectively.

In 2D FE calculations by using first order triangular elements, the nodal forces are easily obtained by computing the stresses $\bar{n} \cdot \bar{\bar{T}}_m^*$ on both sides of the element edges.

By way of illustration, in Fig. 3 some results of a static 2D FE simulation of a 6/4 SRM are shown, viz the flux pattern, the force distribution (nodal forces), and the ensuing
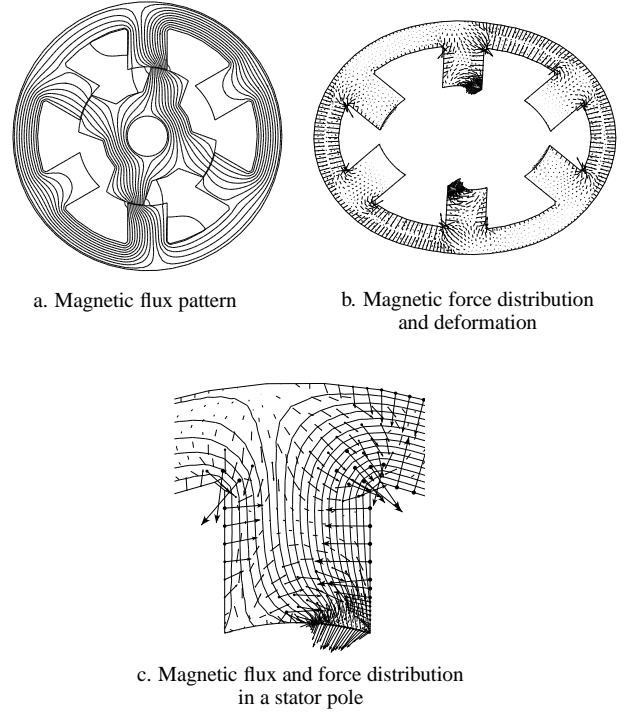
deformation (with a magnification of 2000). The force distribution, shown in Fig. 3.c, clearly consists of both volume and surface forces. The volume forces are (approximately) directed towards the curvature center of the flux lines, as if trying to deform the magnetic material such that the magnetic path length shortens.

B. Structural Analysis and Equations of Motion

Vibrations and the resulting acoustic noise can be reduced if coincidences between the exciting force frequency harmonics and the natural frequencies of the machine structure are avoided. Often it is impossible to avoid such coincidences at all operating points [9].

From the perspective of noise and vibrations, the stators of SRMs can be modelled as a system consisting of a number of masses linked by springs and damping elements, in order to facilitate analytical solution of the dynamic behavior of the structure. The vibration model should transform these distributed parameters into discrete forms, enabling differential equations of motion to be constructed. Alternatively, modal analysis, which is a process of forcing the structure to vibrate mainly at apriori determined resonant frequencies and vibration modes, can also effectively describe the dynamics of the vibrating structure [10, 11, 12].

Prediction of the natural modes and natural frequencies of SRM mechanical structures is very important at the design stage. Analytical models of simplified structures can be formulated relating the resonant frequencies to the geometrical parameters and material properties of the machine [13]. An approximate formulation for the frequency of the fundamental mode can be achieved by modelling the stator lamination stack as a uniform cylindrical shell and using the energy conservation principle in terms of kinetic and poten-

tial energies to deduce the frequency [4]. For relative accuracy, structural finite element analysis for determining the natural modes and frequencies is deployed.

For the analysis of vibrations generated by the magnetic forces, a structural analysis of the SRM stator has been carried out by means of the two-dimensional finite element method. Figs. 4.a-e show some of the computed mode shapes, viz those which can be characterized as a 0th, 2nd and 4th order radial displacement respectively. The outer stator boundary in undeformed state is shown in dashed line.

If mechanical damping is not considered, the equations of motion in the frequency domain are written as follows:

$$-\omega_k^2 \, m_i \, \bar{q}_{ik} + k_i \, \bar{q}_{ik} = \bar{f}_{ik} \qquad (17)$$

where m_i and k_i are the generalized mass and stiffness respectively, and $\bar{q}_{ik}$ and $\bar{f}_{ik}$ are the complex values of the kth time harmonic (pulsation ω_k) of the generalized displacement and force respectively of the ith mode.

C. Dynamic Finite Element Simulations

The procedure for calculating the modal vibrations in a SRM can be summarized as follows. First a series of calculations of the magnetic field, yielding the magnetic force distribution based on the magnetic stress tensor $\bar{\bar{T}}_m^*$ (15), are carried out, where the input consists of the (measured) phase currents or voltages as function of the rotor position. Thanks to the periodicity condition (5) only a twelfth of a rotor revolution ($\frac{1}{12 f_{rot}}$) has to be simulated for a 6/4 SRM. On the basis of the mode shapes, computed by means of a structural FE analysis of the SRM, and the nodal magnetic forces, the generalized forces $f_i(t)$, and further by means of a Fourier analysis, the force components $\bar{f}_{ik}$ are calculated. Finally, the time harmonics of the modal displacements are computed by using (17).

Both FE simulations and measurements have been carried out on a 1.2 kW 6/4 SRM at a speed of 1400 rpm, i.e. f_{rot}=23.33 Hz, f_0 = 93.33 Hz, and operating in single pulse mode. For the simulations, an idealized 6/4 SRM drive, as defined above, and constant speed were assumed. Figs. 4.f-j show the calculated modal displacements for the modes depicted in Figs. 4.a-e. By considering the nonzero order modes in pairs, e.g. the pair 2/2', two modal displacements with the same amplitude and with a phase shift of $\pm 90°$ result in a rotating wave. For instance, a phase lag (lead) of 90° of the modal displacement of mode 2' with respect to mode 2 results in a wave rotating in the same (opposite) direction as the rotor, which corresponds to a spatial order κ_k of 2 (-2). The frequency spectrum and direction of rotation of these waves can be predicted on the basis of (8) for an idealized SRM or (13) in general. The computed frequency spectrum and phase shifts of modes 2 and 2', as shown in Figs. 4.g-h, correspond to the predicted frequency spectrum for spatial ordes 2 and -2 (8). Analogously, the computed results for mode 0 (standing wave) and modes 4/4', shown in Figs. 4.f and 4.i-j respectively, agree with the theoretical results (8), taking into account that, according to (2), spatial orders 4 and -4 are equivalent to orders -2 and 2 respectively.

a. mode 0 ; $f_n = 10.00$ kHz

f. modal displacement - mode 0

b. mode 2 ; $f_n = 1.68$ kHz

g. modal displacement - mode 2/2'

c. mode 2' ; $f_n = 1.68$ kHz

h. phase shift mode 2' - mode 2

d. mode 4 ; $f_n = 7.08$ kHz

i. modal displacement - mode 4/4'

e. mode 4' ; $f_n = 7.08$ kHz

j. phase shift mode 4' - mode 4
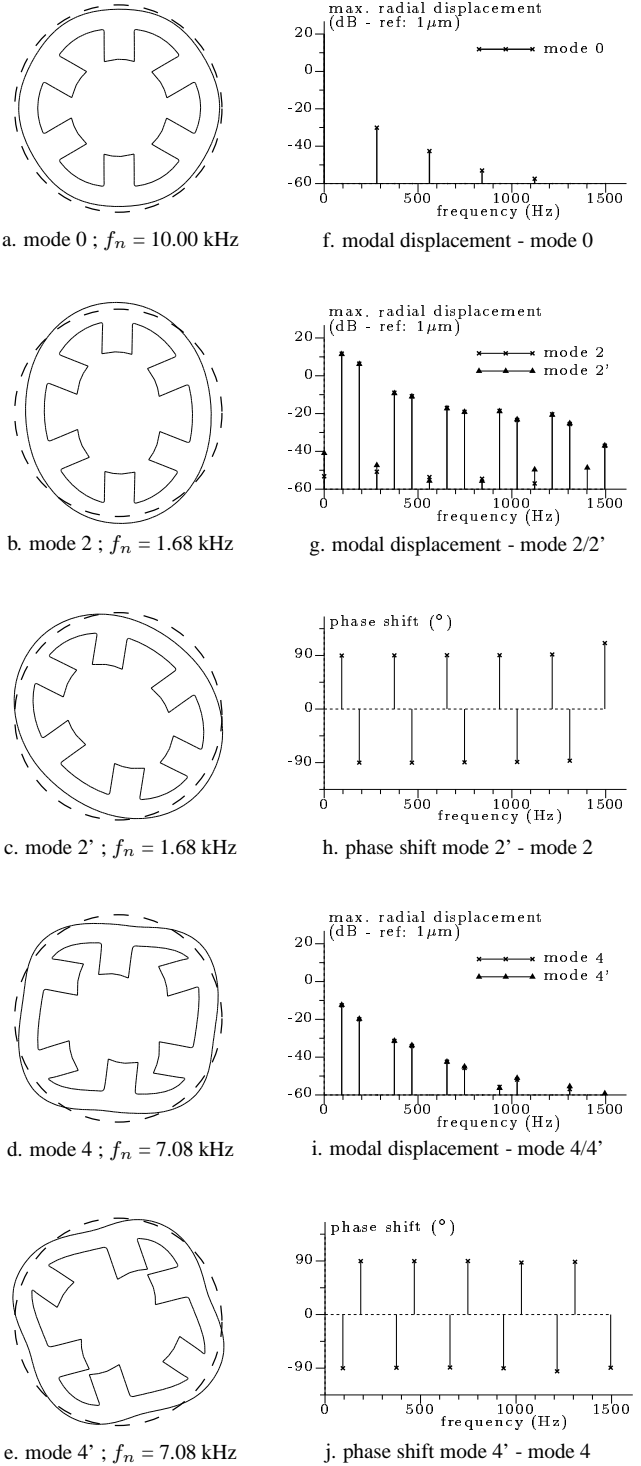
Fig. 4. Computed mode shapes, natural frequencies and modal displacements of a 1.2 kW 6/4 SRM (f_{rot}=23.33 Hz, f_0=93.33 Hz)

4. Experimental Verification

Vibration measurements have been carried out on the 6/4 SRM at a speed of 1400 rpm (f_{rot}=23.33 Hz) and at two load conditions set by controlling the phase currents and the load torque, viz at a set current $I_{set} = 2.0$ A and 7.5 A respectively.

For a set current I_{set}=2.0 A, the torque, which corresponds to force components of zeroth spatial order (κ_k=0),

acceleration (dB - ref: 1 m/s^2)
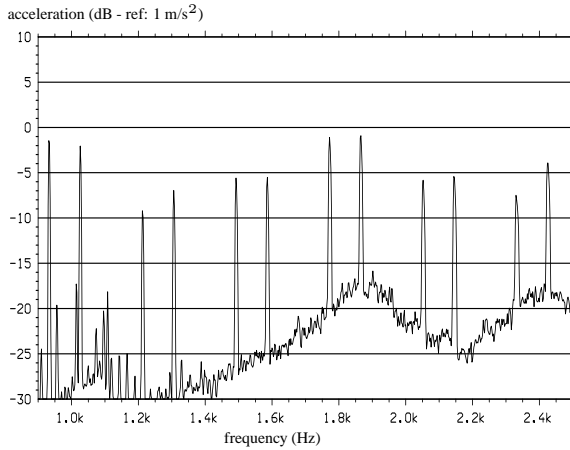
Fig. 5. Measured vibrations (1400 rpm, I_{set}=2.0 A)

acceleration (dB - ref: 1 m/s^2)
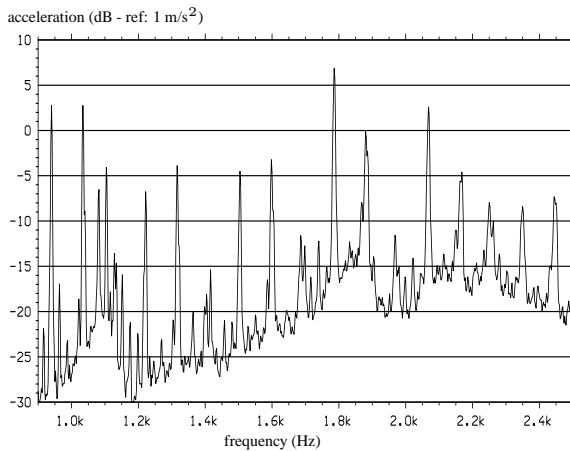
Fig. 6. Measured vibrations (1400 rpm, I_{set}=7.5 A)

is very low (less than 1 Nm). Fig. 5 shows that in this case the frequency spectrum of the vibrations is mainly determined by the time harmonic orders λ_k corresponding to spatial orders $\kappa_k = 2$ and -2, given by (8).

By increasing the load torque and the set current to approximately 8 Nm and 7.5 A respectively, also the frequencies corresponding to $\kappa_k = 0$, viz multiples of $12f_{rot}$, appear in the vibration spectrum, as shown in Fig. 6. Furthermore, some side bands with a frequency step of f_{rot}, which are thus due to rotor asymmetries or load torque ripples, are clearly observed.

5. Conclusion

In this paper a procedure for calculating the vibrations of magnetic origin in switched reluctance motors together with an analytical method for predicting the frequency spectra of the vibration modes have been presented. The modelling method assumed an idealized 6/4 SRM drive and a constant speed. By considering a pair of modes of nonzero order, it was observed that two modal displacements with the same amplitude and a phase shift of $\pm 90^o$, result in a rotating wave. The frequency spectrum and direction of rotation of this wave is predictable by using the analytical method. Experimental verification through vibration measurements, conforms the validity of the devised method. Computed vi-

bration mode shapes, resonance frequencies and modal displacements as well as measured vibrations at different setups are graphically displayed.

References

[1] D. E. Cameron, J. H. Lang, and S. D. Umans, "The origin and reduction of acoustic noise in doubly salient variable-reluctance motors," *IEEE Transactions on Industry Applications*, Vol. 28, Nov./Dec. 1992, pp. 1250–1255

[2] P. Pillay, W. Cai, "An investigation into vibration in switched reluctance motor," *IEEE Transaction on Industrial Applications*, Vol. 35, May/June 1999, pp. 589-596

[3] C.-Y. Wu and C. Pollock, "Analysis and reduction of vibration and acoustic noise in a switched reluctance drive," *IEEE Transactions on Industry Applications*, Vol. 31, pp. 91–98, Jan./Febr. 1995

[4] R. S. Colby, F. M. Mottier, and T. J. E. Miller, "Vibration modes and acoustic noise in a four-phase switched reluctance motor," *IEEE Transactions on Industry Applications*, Vol. 32, Nov./Dec. 1996, pp. 1357–1364

[5] C.G.C. Neves, R. Carlson, N. Sadowski, "Vibrational behavior of switched reluctance motors by simulation and experimental procedures," *IEEE Transactions on Magnetics*, Vol. 34, September 1998, pp. 3158-3161

[6] H. Javadi, Y. Lefèvre, S. Clénet, and M. Lajoie-Mazenc, "Electro-magneto-mechanical characterizations of the vibration of magnetic origin of electrical machines," *IEEE Transactions on Magnetics*, Vol. 31, May 1995, pp. 1892–1895

[7] L. Vandevelde, J. J. C. Gyselinck, and J. A. A. Melkebeek, "Long-Range Magnetic Force and Deformation Calculation using the 2D Finite Element Method," *IEEE Transactions on Magnetics*, Vol. 34, September 1998, pp. 3540-3543

[8] L. Vandevelde and J. A. A. Melkebeek, "Magnetic Forces and Magnetostriction in Ferromagnetic Material," *Compel*, vol. 20, 2001, pp. 32–50

[9] S.P. Verma, A. Balan, "Vibration model for stators of electrical machines incorporating the damping effects," in *Proceedings ELECTRIMACS'96*, September 1996, pp. 755-761

[10] Y. Tang, "Characterization, numerical analysis and design of switched reluctance motors" *IEEE Transactions on Industry Applications*, Vol. 33, No.6 , Nov./Dec. 1997, pp.1544–1552

[11] W. Cai, P. Pillay, "Resonance frequencies and mode shapes of switched reluctance motors," *IEEE Transactions on Energy Conversion*, vol. 16, March 2001, pp. 43-48

[12] J.P. Hong, K.H. Ha, J. Lee, "Stator pole and yoke design for vibration reduction of switched reluctance motor," *IEEE Transaction on Magnetics*, Vol. 38, March 2002, pp. 929-932.

[13] F. Blaabjerg, P. Omand, J.k. Pedersen, "Multidisciplinary Design of Electrical Drives," *Intelligent Motion*, June 1999 Proceedings, pp. 201–210